nadium migration to the particle interior occurs in this system during steaming.

Catalytic evidence shows that the strong acid cracking due to the zeolite is maintained by the catalyst design. In addition, activity and selectivity data in the presence of vanadium indicates that the vanadium trapping function is operative.

Therefore we successfully designed and synthesized a cracking catalyst that combines high zeolitic cracking activity with good vanadium passivation.

Acknowledgment. We thank the Department of Energy, Office of Basic Energy Sciences, Division of Chemical Sciences, and the donors of the Petroleum Research Fund, administered by the American Chemical Society, for partial support of this research through equipment purchase (University of Connecticut).

Registry No. V, 7440-62-2; forsterite, 15118-03-3.

Synthesis, Characterization, and Electropolymerization of Nickel(II) Macrocyclic Compounds Containing Pendant *N*-Alkylpyrrole Substituents

Colin P. Horwitz

Department of Chemistry, Rensselaer Polytechnic Institute, Troy, New York 12180-3590

Received March 8, 1989

Incorporation of pendant *N*-alkylpyrrole moieties onto Ni(II)-containing macrocyclic complexes permits formation of electroactive polymer films that adhere to a Pt electrode surface when the pyrrole moieties are electrochemically oxidized. The polymer films, when placed in solvent and supporting electrolyte with no monomer present, exhibit electrochemical activity resembling the monomer in solution for the Ni(II/III) couple and also voltammetry that corresponds to formation of an *N*-alkylpolypyrrole backbone. The compounds were prepared by reaction of the macrocycle $[Ni[(MeOEthi)_2Me_2[14]tetraeneN_4]]^{2+}$ with 1-(2-aminoethyl)pyrrole, 1-(3-aminopropyl)pyrrole, or 1-(6-aminohexyl)pyrrole. The three different *N*-alkylpyrrole compounds allowed changing the distance between the pyrrole functional group and the macrocycle. The relative rates of electropolymerization and resulting film thicknesses were found to be a function of the alkyl chain length as well as the supporting electrolyte in which the polymer was grown when using acetonitrile as the solvent. Electropolymerization in CH_2Cl_2 showed little dependence on the electrolyte.

The modification of electrode surfaces with transition-metal complex polymer films formed by electropolymerization techniques has received considerable attention in recent years.[1] A variety of potentially practical uses have been suggested for chemically modified electrodes including supported electrocatalysts, solid-state devices, battery electrolytes, and others.[2] Much of the understanding of the fundamental electrochemical properties of polymer-modified electrodes (PMEs) necessary for producing practical devices has been elucidated by utilizing films derived from vinyl-substituted ruthenium and osmium polypyridyl complexes.[3] In conjunction with continuing studies on the electrochemical properties of PMEs, attention is now being been focused on finding new electropolymerizable moieties to replace the vinyl substituents and also new metal complexes. It is likely that some of the future advances in PMEs will come from the preparation of polymer films derived from these new complexes.

Electropolymerizable species that might be generally applicable to transition-metal complex polymer film formation by electropolymerization include pyrrole, aniline, and *N*-alkyl-substituted pyrrole and aniline derivatives. Polypyrrole[4] and polyaniline[5] are well-known electronically conducting polymers formed by oxidative electropolymerization of the corresponding monomers. The *N*-alkyl-substituted aniline species form tail-to-tail coupled dimeric species when oxidized electrochemically,[6] and the presence of two of these substituted aniline groups on a metal complex can lead to polymer film formation.[7] Transition-metal complex polymer films derived from porphyrins,[8] cyclams,[9] Schiff bases,[7] metal polypyridyl complexes,[10] and metallocenes[11] have now been prepared utilizing

(1) (a) Murray, R. W. *Electroanal. Chem.* **1984**, *13*, 191. (b) Murray, R. W.; Ewing, A. G.; Durst, R. A. *Anal. Chem.* **1987**, *59*, 379A. (c) Bard, A. J. *J. Chem. Educ.* **1983**, *60*, 302. (d) Wrighton, M. S. *Science* **1986**, *231*, 32.

(2) Swalen, J. D.; Allara, D. L.; Andrade, J. D.; Chandross, E. A.; Garoff, S.; Israelachvili, J.; McCarthy, T. J.; et al. *Langmuir* **1987**, *3*, 932.

(3) (a) Abruna, H. D.; Denisevich, P.; Umana, M.; Meyer, T. J.; Murray, R. W. *J. Am. Chem. Soc.* **1981**, *103*, 1. (b) Meyer, T. J.; Sullivan, B. P.; Caspar, J. V. *Inorg. Chem.* **1987**, *26*, 4147. (c) Calvert, J. M.; Schmehl, R. H.; Sullivan, B. P.; Facci, J. S.; Meyer, T. J.; Murray, R. W.; *Ibid.* **1983**, *22*, 2151. (d) Guadalupe, A. R.; Usifer, D. A.; Potts, K. T.; Hurrell, H. C.; Mogstad, A.-E.; Abruna, H. D. *J. Am. Chem. Soc.* **1988**, *110*, 3462.

(4) (a) Diaz, A. F.; Castillo, J. I.; Logan, J. A.; Lee, W.-Y. *J. Electroanal. Chem.* **1981**, *129*, 115. (b) Feldman, B. J.; Burgmayer, P.; Murray, R. W. *J. Am. Chem. Soc.* **1985**, *107*, 872. (c) Feldberg, S. *Ibid.* **1984**, *106*, 4671. (d) *Handbook of Conducting Polymers*; Skotheim, T. A., Ed.; Marcel Dekker: New York, 1986.

(5) (a) Wei, Y.; Focke, W. W.; Wnek, G. E.; Ray, A.; MacDiarmid, A. G. *J. Phys. Chem.* **1989**, *93*, 495. (b) Huang, W.-S.; Humphrey, B. D.; MacDiarmid, A. G. *J. Chem. Soc., Faraday Trans. 1* **1986**, *82*, 2385. (c) MacDiarmid, A. G.; Chiang, J. C.; Richter, A. F.; Somasiri, N. L. D. In *Conducting Polymers*; Alcacer, L.; Ed.; Reidel: Dordrecht, Holland, 1987.

(6) (a) Hand, R. L.; Nelson, R. F. *J. Am. Chem. Soc.* **1974**, *96*, 850. (b) Mizoguchi, T.; Adams, R. N. *Ibid.* **1962**, *84*, 2058.

(7) Horwitz, C. P.; Murray, R. W. *Mol. Cryst. Lig. Cryst.* **1988**, *160*, 389.

(8) Bedioui, F.; Merino, A.; Devynck, J.; Mestres, C.-E.; Bied-Charreton, C. *J. Electroanal. Chem.* **1988**, *239*, 433.

(9) Collin, J.-P.; Sauvage, J.-P. *J. Chem. Soc. Chem. Commun.* **1987**, 1075.

0897-4756/89/2801-0463$01.50/0

these electropolymerizable molecules.

We now wish to report the electropolymerization of the macrocyclic complex derived from I, which contains pendant *N*-alkylpyrrole substituents as the polymerizable moiety. Polymer films containing nickel tetraaza mac-

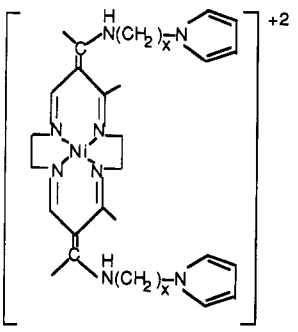

Ia, $x = 2$
Ib, $x = 3$
Ic, $x = 6$

rocycles formed by either electropolymerization or formation of a chemical link between the macrocycle and a preadsorbed polymer film have been described.[9,12,13] The macrocyclic complexes I were chosen because of their relative ease of preparation and derivitization as described by Busch and co-workers.[14] Furthermore, while our initial studies have centered on the nickel-containing macrocycles, the cobalt and iron analogues are among the best oxygen carriers, suggesting the possible application of these films as oxygen sensors or O_2/N_2 separators. We observed in performing this work that the electropolymerization of the monomers derived from I was strongly dependent on the value of x and also the supporting electrolyte–solvent combination.

Experimental Section

Physical Measurements. Infrared spectra were obtained as KBr pellets on a Perkin Elmer 283B infrared spectrophotometer. A Hewlett-Packard HP8452A diode array spectrophotometer controlled with a Zenith 159 personal computer was used for UV–vis spectra. ^{1}H NMR spectra were recorded by using either a Varian XL-200 or an IBM WP-100 SY spectrometer. Elemental analyses were performed by Robertson Laboratory, Madison, NJ.

Electrochemistry. Electrochemical measurements were obtained by using an EG&G Princeton Applied Research Model 273 potentiostat/galvanostat controlled with the Zenith personal computer and the Headstart (PARC) software package and recorded on a Graphtec WX 1200 XY recorder. Voltammograms were obtained in the three-electrode mode by using Pt disk electrodes ($A \sim 0.15$ cm^2) shrouded in Teflon (polished with 1-μm diamond paste (Buehler) prior to use), a Pt wire as counter electrode, and either a SSCE (sodium chloride saturated calomel electrode) or a Ag wire as reference or pseudoreference electrodes respectively. The supporting electrolytes [(*n*-Bu)$_4$N][BF$_4$] (Fluka puriss), [(*n*-Bu)$_4$N][PF$_6$] (Fluka puriss), [(*n*-Bu)$_4$N][CH$_3$C$_6$H$_4$SO$_3$] (Aldrich), and [(*n*-Bu)$_4$N][ClO$_4$] (VWR "Baker") were purified by using standard procedures. The [(*n*-Bu$_4$)N][CF$_3$SO$_3$] was prepared according to the procedure described in the literature. The CH$_3$CN (Burdick and Jackson) was used as received. CH$_2$Cl$_2$ was distilled under N$_2$ from P$_4$O$_{10}$. All polymer films were grown in a Vacuum Atmospheres glovebox under an N$_2$ atmosphere.

Materials. All chemicals necessary for the synthesis of the nickel macrocycle I and the *N*-alkyl-substituted pyrrole derivatives were of reagent grade (Aldrich) and were used without further purification. The macrocyclic complexes and (Ni(Ac$_2$Me$_2$[14])-tetraeneN$_4$) and [Ni[(MeOEthi)$_2$Me$_2$[14]tetraeneN$_4$]][PF$_6$]$_2$ were prepared according to procedures described in the literature,[15] and the purity was checked by ^{1}H NMR spectroscopy.

Synthesis of 1-(2-(Acetylamino)ethyl)pyrrole (IIa), 1-(3-(Acetylamino)propyl)pyrrole (IIb), and 1-(6-(Acetylamino)hexyl)pyrrole (IIc). All of these compounds were prepared in a similar manner, so only the synthesis of IIa is described. The following is a modification of the procedure described by Jirkovsky and Baudy.[16] A mixture was prepared containing 2,5-dimethoxytetrahydrofuran (25 mL, 0.19 mol), glacial acetic acid (160 mL) and 1,4-dioxane (225 mL). To this solution was added dropwise ethylenediamine (12.8 mL, 0.19 mol). The solution was heated under reflux for 4 h and then stirred at room temperature overnight. Volatiles are removed under reduced pressure, resulting in a viscous brown–black residue. The residue was dissolved in chloroform (80 mL), and 1-mL aliquots of a 10% sodium bicarbonate solution were added with swirling until no gas evolution was observed. The organic phase was separated, dried with MgSO$_4$, filtered, and evaporated to give a dark brown–black viscous residue. The residue was dissolved in CH$_2$Cl$_2$ and loaded onto a silica gel column for flash chromatography. Two impurities were eluted with 1:1 CH$_2$Cl$_2$:hexane. The product moved slowly with this solvent system, so care must be taken not to lose product. The product was washed off the column with THF, and the eluent was collected and evaporated to give a light brown solid, 40–50% yield [^{1}H NMR (CDCl$_3$) δ 6.63 (2 H, tr, J = 2 Hz), 6.15 (2 H, tr, J = 2 Hz), 5.78 (1 H, s) 3.99 (2 H, tr, J = 6.3 H), 3.52 (2 H, tr, J = 6.3 Hz) 1.93 (1 H, s)]. The longer chain compounds are both viscous liquids. These compounds are difficult to purify and were hydrolyzed to the amine, synthesis below, immediately after their preparation.

Synthesis of 1-(2-Aminoethyl)pyrrole (IIIa), 1-(3-Aminopropyl)pyrrole (IIIb), and 1-(6-Aminohexyl)pyrrole (IIIc). All of these compounds were prepared according to the procedures described by Jirkovsky and Baudy,[16] so only the synthesis of IIIa is described. Compound IIa, 5.3 g, was added to a 10% aqueous KOH solution, 100 mL, and the solution was heated to reflux for 2 h. After cooling, the solution was extracted with two 100-mL portions of CDCl$_3$, and the chloroform extracts were combined and then washed with 75 mL of aqueous 10% HCl. The aqueous acid solution was rendered basic (pH ~10) with 30% aqueous NaOH and extracted with two 75-mL aliquots of CDCl$_3$, and the chloroform was removed in vacuo, yielding essentially pure product. ^{1}H NMR (CDCl$_3$) δ: compound IIIa 6.69 (tr, 2 H, J = 2 Hz), 6.17 (tr, 2 H, J = 2 Hz), 3.94 (tr, 2 H, J = 6 Hz), 3.04 (tr, 2 H, J = 6 Hz), 1.28 (s, 2 H); compound IIIb 6.64 (tr, 2 H, J = 2 Hz), 6.13 (tr, 2 H, J = 2 Hz), 3.94 (tr, 2 H, J = 6.9 Hz), 2.67 (tr, 2 H, J = 6.8 Hz), 1.93–1.44 (m, 2 H), 1.30 (s, 2 H); compound IIIc 6.62 (tr, 2 H, J = 2 Hz), 6.12 (tr, 2 H, 2 Hz), 3.85 (tr, 2 H, J = 7 Hz), 2.65 (tr, 2 H, J = 6.4 Hz), 1.8–1.2 (m, 8 H), 1.1 (s, 2 H).

Synthesis of [2,11-Dimethyl-3,10-bis[1-(1-(2-aminoethyl)-pyrrole)ethylidene]-1,5,8,12-tetraazacyclotetradeca-1,4,8,11-tetraene]nickel(II) Hexafluorophosphate ([Ni[(*N*-ethylpyrroleNHEthi)$_2$Me$_2$[14]tetraeneN$_4$]][PF$_6$]$_2$, Ia). [Ni-

(10) (a) Bidan, G.; Deronzier, A.; Moutet, J.-C. *Nouv. J. Chim.* **1984**, *8*, 501. (b) Cosnier, S.; Deronzier, A.; Moutet, J.-C. *J. Electroanal. Chem.* **1985**, *193*, 193. (c) Downard, A. J.; Surridge, N. A.; Meyer, T. J.; Cosnier, S.; Deronzier, A.; Moutet, J.-C. *Ibid.* **1988**, *246*, 321. (d) Daire, F.; Bedioui, F.; Devynck, J.; Bied-Charreton, C. *Ibid.* **1987**, *224*, 95. (e) Eaves, J. G.; Munro, H. S.; Parker, D. *Inorg. Chem.* **1987**, *26*, 644–650. (f) Cosnier, S.; Deronzier, A.; Moutet, J.-C. *J. Phys. Chem.* **1985**, *89*, 4895.

(11) (a) Inagaki, T.; Hunter, X. Q.; Skotheim, T. A.; Okamoto, Y. *J. Chem. Soc., Chem. Commun.* **1988**, 126. (b) Haimerl, A.; Merz, A. *Angew. Chem., Int. Ed. Engl.* **1986**, *25*, 180.

(12) Bailey, C. L.; Bereman, R. D.; Rillema, D. P.; Nowak, R. *Inorg. Chem.* **1986**, *25*, 933.

(13) Ellis, C. D.; Meyer, T. J. *Inorg. Chem.* **1984**, *23*, 1748.

(14) (a) Busch, D. H. *Pure Appl. Chem.* **1980**, *52*, 2477. (b) Streeky, J. A.; Pillsbury, D. G.; Busch, D. H. *Inorg. Chem.* **1980**, *19*, 3148. (c) Schammel, W. P.; Zimmer, L. L.; Busch, D. H. *Ibid.* **1980**, *19*, 3159. (d) Korybut-Daszkiewicz, B.; Kojima, M.; Cameron, J. H.; Herron, N.; Chavan, M. Y.; Jircitano, A. J.; Coltrain, B. K.; Neer, G. L.; Alcock, N. W.; Busch, D. H. *Ibid.* **1984**, *23*, 903. (e) Caste, M. L.; Cairns, C. J.; Church, J.; Lin, W.-K.; Gallucci, J. C.; Busch, D. H. *Ibid.* **1987**, *26*, 78. (f) Cameron, J. H.; Kojima, M.; Korybut-Daszkiewicz, B.; Coltrain, B. K.; Meade, T. J.; Alcock, N. W.; Busch, D. H. *Ibid.* **1987**, *26*, 427. (g) Herron, N.; Chavan, M. Y.; Busch, D. *J. Chem. Soc., Dalton Trans.* **1984**, 1491. (h) Herron, N.; Grzybowski, J. J.; Matsumoto, N.; Zimmer, L. L.; Christoph, G. G.; Busch, D. H. *J. Am. Chem. Soc.* **1982**, *104*, 1999.

(15) Riley, D. P.; Busch, D. H. *Inorg. Synth.* **1978**, *18*, 36.

(16) Jirkovsky, I.; Baudy, R. *Synthesis* **1981**, 481.

Table I. Spectroscopic and Electrochemical Data

compound	^{1}H NMR chem shifts[a-d]	abs max λ_{max}, nm (ϵ, M^{-1} cm^{-1})[e]	$E°$, V (ΔE_p, mV)[f]
Ni[14]C2pyrrole	7.89 (s, 1 H), 6.80 (tr, 2 H, 2 Hz), 6.01 (tr, 2 H, 2 Hz), 4.35 (tr, 2 H, 5.1 Hz), 4.11 (tr, 2 H, 5.1 Hz), 3.52 (s, 4 H), 2.28 (s, 3 H), 2.15 (s, 3 H)	282 (20 800); 402 (36 800); 490 (2200)	1.02 (80)
Ni[14]C3pyrrole	7.96 (s, 1 H), 6.74 (tr, 2 H, 2 Hz), 6.03 (tr, 2 H, 2 Hz), 4.1 (tr, 2 H, 6.7 Hz), 3.7 (tr, 2 H, 7 Hz), 3.5 (s, 4 H), 2.54 (s, 3 H), 2.41 (s, 3 H), 2.3–2.1 (m, 2 H)	278 (18 700); 400 (35 400); 480 (1470)	0.99 (90)
Ni[14]C6pyrrole	7.97 (s, 1 H), 6.66 (tr, 2 Hz), 5.98 (tr, 2 H, 2 Hz), 3.9 (tr, 2 H, 7 Hz), 3.71 (tr, 2 H, 7.1 Hz), 3.54 (s, 4 H), 2.60 (s, 3 H), 2.42 (s, 3 H), 1.8 (m, 4 H), 1.4 (m, 4 H)	280 (19 400); 398 (33 400); 480 (1550)	0.97 (90)

[a] Values relative to external Me_4Si. [b] Acetone-d_6. [c] Values in parentheses are multiplicity, number of protons, coupling constant. [d] Amine protons not observed. [e] Acetonitrile. [f] Potentials versus SSCE with Pt disk working electrode and sweep rate 100 mV/s; CH_3CN solution with $[(n\text{-}Bu)_4N][ClO_4]$ supporting electrolyte.

$[(MeOEthi)_2Me_2[14]tetraeneN_4]][PF_6]_2$ (250 mg, 0.37 mmol) was dissolved in 10 mL of CH_3CN, and 1-(2-aminoethyl)pyrrole (160 mg, 1.5 mmol) dissolved in 5 mL of CH_3CN was added. The solution immediately changed from yellow-brown to red-brown upon addition of IIIa. The acetonitrile was removed in vacuo, and the resulting solid redissolved in hot methanol (35 mL) and filtered through a coarse porosity frit. The solution volume was reduced to approximately 15 mL, and the solution was cooled to 0 °C for approximately 1 h. The precipitate was collected by filtration, washed with diethyl ether, and air dried. Anal. Calcd for $C_{28}H_{40}N_8NiP_2F_{12}$: C, 40.16; H, 4.82; N, 13.38. Found: C, 40.28; H, 4.69; N, 13.01.

Synthesis of [2,11-Dimethyl-3,10-bis[1-(1-(3-aminopropyl)pyrrole)ethylidene]-1,5,8,12-tetraazacyclotetradeca-1,4,8,11-tetraene]nickel(II) Hexafluorophosphate ([Ni[(*N*-propylpyrroleNHEthi)$_2$Me$_2$[14]tetraeneN$_4$]][PF$_6$]$_2$, Ib) and [2,11-Dimethyl-3,10-bis[1-(1-(6-aminohexyl)pyrrole)ethylidene]-1,5,8,12-tetraazacyclotetradeca-1,4,8,11-tetraene]nickel(II) Hexafluorophosphate ([Ni[(*N*-hexylpyrroleNHEthi)$_2$Me$_2$[14]tetraeneN$_4$]][PF$_6$]$_2$, Ic). To a 10-mL CH_3CN solution containing $[Ni[(MeOEthi)_2Me_2[14]tetraeneN_4]][PF_6]_2$ (250 mg, 0.37 mmol) was added either 1-(3-aminopropyl)pyrrole (160 mg, 1.5 mmol) or 1-(6-hexylamino)-pyrrole (290 mg, 1.5 mmol). The solution immediately changed from yellow-brown to red-brown upon addition of the amine. The acetonitrile was removed in vacuo until approximately 1 mL remained, whereupon 5 mL of CH_3OH was added. Diethyl ether (30 mL) was added to the CH_3CN/CH_3OH solution, resulting in the formation of a turbid solution. The solution was maintained at 0 °C for 2 h, whereupon an orange solid precipitated. The solid was recovered by filtration, washed with diethyl ether, and air dried. Product yields were generally in the 60–75% range. Anal. Calcd for $C_{30}H_{44}N_8NiP_2F_{12}$ (Ib): C, 41.64; H, 5.12; N, 12.95. Found: C, 43.63; H, 5.18; N, 12.84. Anal. Calcd for $C_{36}H_{56}N_8NiP_2F_{12}$ (Ic): C, 45.54; H, 5.95; N, 11.80. Found: C, 45.70; H, 5.91; N, 11.87.

Results and Discussion

Synthesis and Characterization of the Macrocyclic Complexes. Preparation of the pyrrole-substituted macrocycle complexes Ia, Ib, Ic was performed in accordance with procedures described in the literature for analogous compounds (eq 1).[14] The complexes are designated as Ni[14]C2pyrrole (Ia), Ni[14]C3pyrrole (Ib), and Ni[14]C6pyrrole (Ic) to facilitate further discussion. The reaction was monitored by UV–vis spectroscopy with all three complexes displaying essentially identical spectra (Table I). In all instances the product could be isolated in greater than 60% yield. The solubility in methanol is the most notable difference between the three complexes,

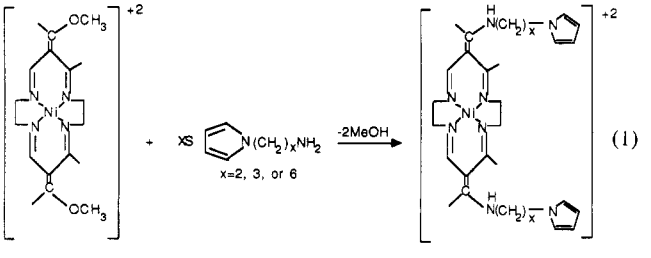

(1)

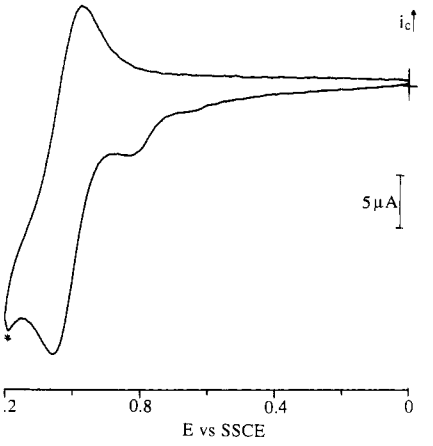

Figure 1. Cyclic voltammogram of a 1.6 mM solution of Ni[14]C2pyrrole; v = 100 mV/s, 0.1 M $[(n\text{-}Bu)_4N][ClO_4]/CH_3CN$, Pt electrode, and E vs SSCE.

increasing in the order Ni[14]C2pyrrole < Ni[14]C3pyrrole < Ni[14]C6pyrrole. Thus complex Ni[14]C2pyrrole could be isolated from methanol by cooling to 0 °C while it was necessary to add ether to a methanol solution containing Ni[14]C3pyrrole and Ni[14]C6pyrrole to precipitate the products. Described in the Experimental Section is a better method for isolating the macrocyclic complexes with the longer alkyl chains.

Addition of the *N*-alkylpyrrole substituents to the macrocycle and the high symmetry of the macrocycles are confirmed in the ^{1}H NMR spectra of the three compounds (Table I). Common features in the ^{1}H NMR spectra include (i) two sets of triplets at approximately δ 6.8 and δ 6.1 assigned to the pyrrole protons, (ii) a triplet ranging from δ 3.9 (Ni[14]C2pyrrole) to 4.35 (Ni[14]C6pyrrole) corresponding to the CH_2 nearest the pyrrole nitrogen, and (iii) a triplet ranging from δ 3.7 (Ni[14]C2pyrrole) to 4.1 (Ni[14]C6pyrrole) arising from the CH_2 farthest from the pyrrole nitrogen. All chemical shift assignments pertaining to the macrocycle are similar to those reported for analogous compounds described in the literature.[14] The infrared spectrum for each of the complexes exhibits a sharp band at 3450 cm^{-1}, indicative of a free N–H stretch, and a broad absorption at 1650–1500 cm^{-1} for the C=C and C=N stretches, and the $[PF_6]^-$ anion has a strong broad band at 830 cm^{-1}. The UV–vis spectra in CH_3CN are essentially identical for the three macrocyclic complexes (Table I).

Electrochemistry. Nickel macrocycle complexes with simple amine substituents analogous to Ia, Ib, and Ic often exhibit a reversible metal-centered redox couple at 1 V vs SSCE.[14] The electrochemical response for a solution containing Ni[14]C2pyrrole at potentials negative of the onset of electropolymerization is shown in Figure 1; measurements were obtained on a polished Pt disk electrode (A = 0.15 cm^2) in CH_3CN solvent with 0.1 M $[(n\text{-}Bu)_4N][ClO_4]$ as the supporting electrolyte and a SSCE reference electrode. The formal potential, $E°$, is 1.02 V

and the peak separation, ΔE_p, is 80 mV. Table I contains the $E°$ values for the three complexes prepared here.

The prewave at approximately 820 mV, Figure 1, may arise from adsorption effects;[17] it does not occur when using $[PF_6]^-$ or $[SO_3CF_3]^-$ as the supporting electrolyte anions. A voltammogram of $[Ni[(PropylNHEthi)_2Me_2[14]tetraeneN_4]]^{2+}$ (propylamine replaces the 1-(2-aminoethyl)-pyrrole, IIIa, in eq 1) also displays a similar prewave under conditions analogous to those sited in Figure 1. Therefore it is unlikely that the wave at 820 mV in Ni[14]C2pyrrole arises from oxidation of the pyrrole moieties. The feature denoted with an asterisk in Figure 1 is, we believe, formation of the pyrrole radical cation. A potential scan to 1.35 V vs SSCE for $[Ni[(PropylNHEthi)_2Me_2[14]tetraeneN_4]]^{2+}$ shows no analogous oxidation.

Polymer Films. The basic properties of polymer film formation and the resulting electrochemistry of the polymer films are essentially identical for the three different complexes. Therefore, the electrochemistry for Ni[14]-C2pyrrole will be discussed in detail. The most notable difference between the three complexes is the rate of electropolymerization, which depends on both the monomer and the anion used for the supporting electrolyte. The specific effects of the monomer and supporting electrolyte anion are described following the more general discussion of film formation and polymer film electrochemistry.

Electropolymerization. The transition-metal complex polymer films were grown in a N_2-filled glovebox in which the water and oxygen contents were maintained at less than 5 ppm. A silver wire was used as a pseudoreference electrode for all experiments in the glovebox. Use of the silver wire pseudoreference electrode shifts the $E°$ for the Ni(II/III) couple approximately 100–200 mV to more positive potentials. To maintain consistency with regard to reporting potentials applied during electropolymerization, all values are referenced relative to the potential at the peak current for the Ni(II/III) oxidation wave, $E_{p,ox,Ni(II/III)}$.

Attempts to prepare the polymers outside the glovebox resulted in the formation of very thin films that showed a rapid decrease in electrochemical response during polymerization. It is not clear whether polymerization was impeded by trace quantities of water or oxygen. Thorough degassing of the electrochemical cell with N_2 did not appear to help maintain a reasonable rate of polymerization, and thus water appears to function to inhibit the polymerization. However when polypyrrole films are grown from acetonitrile solutions, water sometimes is added.[10,18]

Pyrrole and *N*-alkyl-substituted pyrroles electropolymerize when potentials of approximately 0.8 V vs SCE are applied to an electrode immersed in a CH_3CN solution containing the monomer.[4] It was anticipated that a similar situation would apply for the complexes prepared here. However, owing to the cationic nature of the macrocyclic complexes we expected that application of slightly more positive potentials might be required for polymerization. Indeed transition-metal complex polymer films could be grown by successively cycling the potential at least 50 mV past the Ni(II/III) oxidation current peak. As mentioned above, potential excursions 50–100 mV beyond $E_{p,ox,Ni(II/III)}$ result in the oxidation of the pendant pyrrole moieties. Polymerization did not appear to occur if the applied potentials were not past the redox couple for the metal.

(17) Bard, A. J.; Faulkner, L. F. *Electrochemical Methods*; Wiley: New York, 1980.

(18) Γ_{app} determined from the equation $\Gamma_{app} = Q/(nFA)$, where Q is the charge (area) under the reduction wave, n is the number of electrons per metal site ($n = 1$), F is Faraday's constant, and A is electrode area in cm^2.

Scheme I

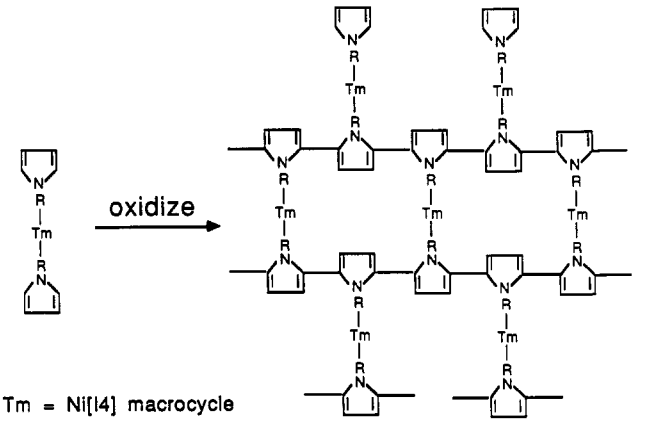

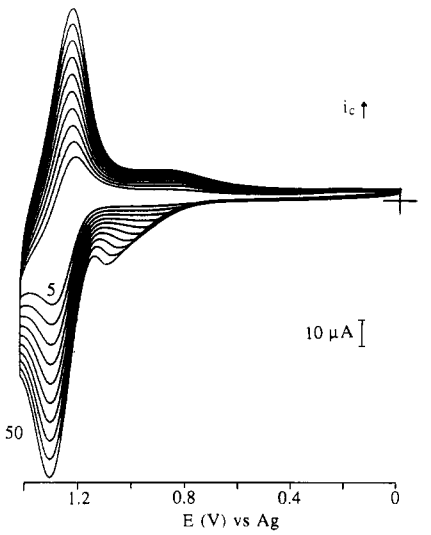

Figure 2. Electropolymerization of 1.0 mM solution of Ni[14]-C2pyrrole; υ = 100 mV/s, 0.1 M $[(n\text{-}Bu)_4N][ClO_4]/CH_3CN$, E vs Ag, and scan range from 0 to 1.45 V [150 mV past the Ni(II/III) oxidation]. Scans 5–50 in increments of 4 unrecorded scans are shown.

An idealized structure for the polymer film is shown in Scheme I; however, defects in the polymer chains are also likely to occur.

The most rapid polymerization rates were observed when the applied potentials were 100–200 mV past the oxidation of the metal center. The faster polymer film growth rate likely arise from the longer time periods spent in the oxidative regime. Polymer films could also be grown by maintaining a constant potential positive of the Ni-(II/III) couple. However, we chose to use the repetitive cycling method to form the polymer films since this should give a clearer indication if any unusual behavior occurred during electropolymerization.

Shown in Figure 2 is the electropolymerization, 50 repetitive potential scans, of a solution containing Ni[14]-C2pyrrole in CH_3CN with 0.1 M $[(n\text{-}Bu)_4N][ClO_4]$ as the supporting electrolyte. Successive potential cycling generates a potential–current curve for the Ni(II/III) couple which increases monotonically in both the oxidative and reductive current directions. A slight increase in the ΔE_p also occurs during polymerization. New, broad oxidation and reduction waves also appear negative of the metal waves with the repetitive cycling.

The oxidation current for the new electroactive species shows a monotonic increase while the reducing current

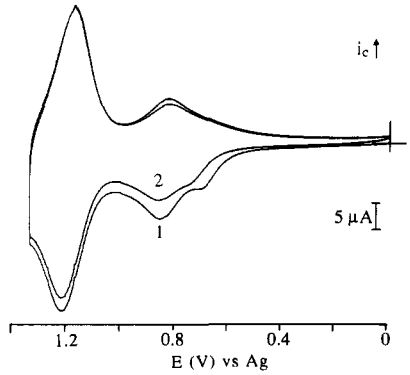

Figure 3. Voltammetric response of poly-Ni[14]C2pyrrole (Γ_{app} = 5.6 × 10^{-9} mol/cm^2) in 0.1 M [(n-Bu)$_4$N][ClO$_4$]/CH$_3$CN at 50 mV/s. Potentials are vs Ag wire. Curve marked 1 is the first scan following polymerization, and that designated 2 is the second scan.

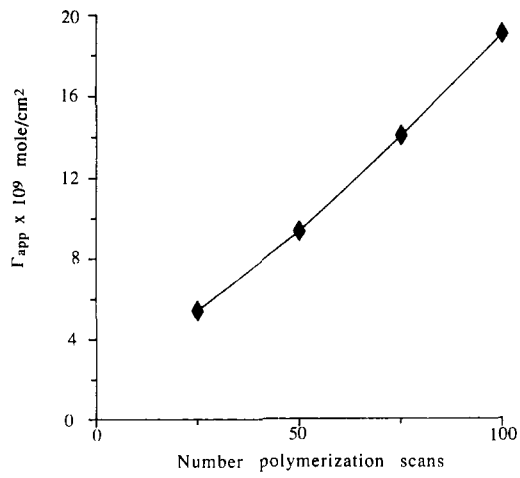

Figure 4. Apparent surface coverage (Γ_{app}) vs number of polymerization scans. Coverage determined at υ = 50 mV/s in 0.1 M [(n-Bu)$_4$N][ClO$_4$]/CH$_3$CN. Polymer films were grown from a 1.3 mM solution of Ni[14]C2pyrrole in 0.1 M [(n-Bu)$_4$N][ClO$_4$]/CH$_3$CN, υ = 100 mV/s, E vs Ag, and scan range from 0 to 1.38V [120 mV past the Ni(II/III) oxidation].

exhibits slower and less sustained growth. Oxidative degradation of the macrocyclic ligand followed by coupling of monomer units does not occur at these potentials as [Ni[(PropylNHEthi)$_2$Me$_2$[14]tetraeneN$_4$]]$^{2+}$ showed no signs of polymer film formation under similar conditions. Some similar tetraaza type macrocycles do form electropolymerized films by direct oxidative coupling of the macrocycles.[12] These new, broad peaks do appear in the region expected for the oxidation/reduction of N-alkyl-substituted polypyrroles (the redox waves for N-alkylpolypyrroles are typically shifted far positive of polypyrrole).[19] The oxidation wave also displays a constant shift to positive potentials as the number of scans increases eventually becoming nearly coincident with the Ni(II/III) oxidation wave. Under the conditions cited in Figure 2 polymer films can be continuously formed through approximately 100 potential scans before a significant decrease in the rate of oxidative and reductive current growth is observed for the metal center. This is also the point at which the pyrrole/polypyrrole oxidation and the Ni(II) oxidation become coincident. The color of the polymer on the electrode depends on the thickness because of interference effects. Relatively short (<25 scans) polymerization times yield golden films while thicker films are purple or green.

Polymer Film Electrochemistry. Upon transfer of the film-coated electrode to a CH$_3$CN solution containing only supporting electrolyte, 0.1 M [(n-Bu)$_4$N][ClO$_4$], and no monomer, an electrochemical response is observed (−0.25 to 1.45 V vs Ag) which is reminiscent of the Ni(II/III) redox process for the monomer in solution (Figure 3). The voltammogram shown in Figure 3 is for the first two scans following transfer to the fresh electrolyte solution. The broad waves associated with the polypyrrole are also observed in the voltammogram. These results demonstrate that electroactivity is maintained for both the Ni(II/III) couple and the polypyrrole. Furthermore, the macrocyclic complex is not degraded during the polymerization reaction. No other electrochemically active species are detected out to −0.75 V, while scanning more positively than 1.45 V results in a large, electrochemically irreversible oxidation wave probably arising from decomposition of the macrocycle.[14]

As expected for thin-film electrochemistry[1a] the shape of the current–potential curve for the Ni(II/III) couple is nearly symmetrical even up to scan rates of 200 mV/s. The wave shape does show signs of diffusional tailing at υ = 500 mV/s. The peak splitting for the metal-centered couple, although not the ideal 0 mV, ranges from 10 mV for thin films to 100 mV for thicker films at υ = 50 mV/s. The theoretical peak width at half-height for thin-film electrochemistry should be 90.6/n mV (n = number of electrons) and independent of scan rate.[1a] The observed widths are 120 and 180 mV at υ = 20 and 500 mV/s, respectively. These data are consistent with thin-film electrochemistry at scan rates below 100 mV/s; however, for the faster scan rates the electrochemistry begins to resemble diffusional behavior[17] and can no longer be accurately described by the equations governing thin-film electrochemistry.

Apparent surface coverages, Γ_{app} (mol/cm^2), were determined by measuring the charge under the Ni(III/II) reduction wave and assuming that the current is generated only by the Ni center.[18] Any contribution from the polypyrrole is ignored. Justification for this approach to calculating Γ_{app} is discussed below. The Γ_{app} is a linear function of the number of repetitive polymerization scans when the potential is scanned at 50 mV/s (Figure 4). Γ_{app} also is roughly independent of scan rate for film coverages ranging from 9 × 10^{-9} to 1.9 × 10^{-8} mol/cm^2 up to υ = 100 mV/s. Faster scan rates and thicker films result in coverages that do not obey thin-film approximations.

The electrochemistry of polypyrrole and N-alkyl-substituted polypyrroles generally exhibit a reasonably well-defined oxidation wave with large capacitive background currents occurring positive of the oxidation peak.[4,20] The reduction current is often broad and featureless. Oxidation of the polypyrrole portion of the transition-metal complex polymer films described here results in generation of the two broad peaks as seen in Figure 3 especially for the thinner films. Thicker films show only the more positive oxidative wave. Two oxidation waves have also been noted for polypyrrole in [(n-Bu)$_4$N][ClO$_4$]/CH$_3$CN.[4a] Interaction of the anion with the delocalized π-cation of the oxidized polypyrrole, ion pairing, and triplet ions have been suggested as possible explanations for the presence of the two oxidation waves. A well-developed reduction wave is ob-

(19) (a) Diaz, A. F.; Kanazawa, K. K.; Gardini, G. P. *J. Chem. Soc., Chem. Commun.* **1979**, 635. (b) Street, G. B.; Lindsey, S. E.; Nazzal, A. J.; Wynne, K. J. *Mol. Cryst. Liq. Cryst.* **1985**, *118*, 137. (c) Downard, A. J.; Pletcher, D. *J. Electroanal. Chem.* **1986**, *206*, 139.

(20) (a) Diaz, A. F.; Castillo, J.; Kanazawa, K. K.; Logan, J. A.; Salmon, M.; Fajardo, O. *J. Electroanal. Chem.* **1982**, *133*, 233. (b) Cross, M. G.; Walton, D.; Morse, N. J.; Mortimer, R. J.; Rosseinsky, D. R.; Simmonds, D. J. *Ibid.* **1985**, *189*, 389.

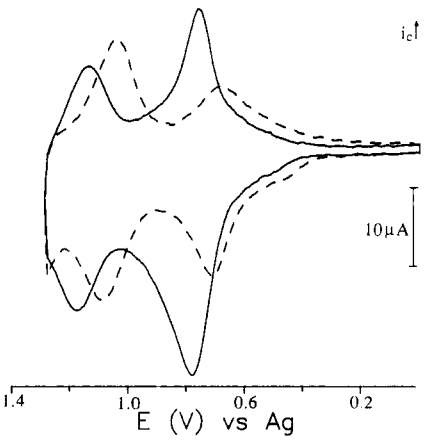

Figure 5. Voltammetric response at 50 mV/s of poly-Ni[14]-C2pyrrole (Γ_{app} = 3 × 10^{-9} mol/cm^2) in (---) 0.1 M [(n-Bu)$_4$N][ClO$_4$]/CH$_3$CN and (—) 0.1 M [(n-Bu)$_4$N][BF$_4$]/CH$_3$CN; E vs Ag.

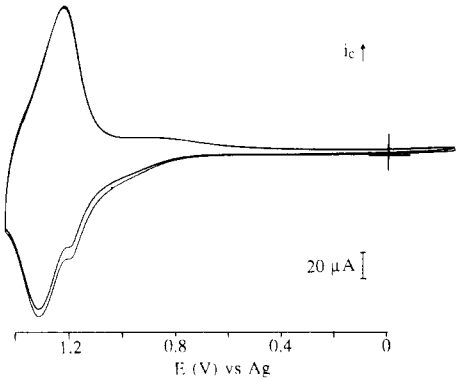

Figure 6. Voltammetric response of poly-Ni[14]C6pyrrole (Γ_{app} = 2.65 × 10^{-8} mol/cm^2) in 0.1 M [(n-Bu)$_4$N][ClO$_4$]/CH$_3$CN at 50 mV/s (E vs Ag). Note the coalescence of the polypyrrole oxidation with the Ni(II/III) oxidation wave; compare with Figure 3.

served under most circumstances for the polymer films prepared from the nickel macrocyclic complexes. However, when apparent surface coverages approach 1 × 10^{-8} mol/cm^2, the reduction broadens into a featureless wave. The general features associated with the polypyrrole electrochemistry in the thin films suggest a moderate degree of ordering for this portion of the film. Broadening of the polypyrrole current–potential behavior in thick polymer films of the three macrocyclic complexes can be explained by an increase in disorder of the backbone much like that observed for thick films of polypyrrole and its N-alkyl derivatives.

The supporting electrolyte in which the polymer film was examined can markedly affect the polypyrrole electrochemistry. Shown in Figure 5 are the current–potential curves for a poly-Ni[14]C2pyrrole film in [(n-Bu)$_4$N][ClO$_4$] and [(n-Bu)$_4$N][BF$_4$] media; the film was grown in [BF$_4$]$^-$ supporting electrolyte. The apparent shift in potential for the Ni(II/III) couple and polypyrrole arise from use of the Ag pseudoreference electrode. If the data are calibrated with respect to ferrocene, the potentials in the two electrolytes are nearly coincident. The Γ_{app} determined from the Ni(II/III) reduction is independent of the electrolyte, Γ_{app} = 3 × 10^{-9} mol/cm^2. The quantity of polypyrrole electrochemically accessed appears to be significantly larger in the tetrafluoroborate electrolyte. The charge, Q, under the reduction wave in [BF$_4$]$^-$ electrolyte is 6 × 10^{-5} C, while the corresponding wave in perchlorate electrolyte is roughly Q = 3 × 10^{-5} C. A similar difference is apparent for the oxidation waves ([BF$_4$]$^-$) Q = 1 × 10^{-4} C and ([ClO$_4$]$^-$) Q = 7 × 10^{-5} C. Anion effects on polypyrrole electrochemistry have been reported, but the differences are not as pronounced as seen in these metal complex polymer films for the analogous anions.[21] Thicker films do not exhibit as pronounced differences when the two different electrolytes are present. The sharpening or broadening of the polypyrrole waves can be reversed by taking the coated electrode from one supporting electrolyte to the other. Sharp, well-defined waves for polypyrrole are not commonly observed because it is assumed that a large variety of polymer morphologies exist in the film. The observed results suggest that under appropriate conditions disordered transition-metal complex polymer films can be partially ordered.

The poly-Ni[14]C2pyrrole film grown under the conditions described in Figure 2 can be cycled at 50 mV/s for 25 scans between the potential limits of −0.25 and 1.45 V vs Ag wire with approximately 10% decrease in both the oxidative and reductive currents associated with the Ni center. The waves assigned to the polypyrrole portion also display a similar but more rapid current decrease. Eventually the film becomes electroinactive if potential cycling is continued for extended time periods. Neither slower or faster scan rates (20–100 mV/s) markedly affect the overall electrochemical properties of the film. Thin films, Γ_{app} < 10^{-9} mol/cm^2, show more rapid loss of electroactivity. Changing the supporting electrolyte to any of the anions mentioned above does not help to maintain electroactivity. However when [(n-Bu)$_4$N][CH$_3$C$_6$H$_4$SO$_3$] was used as the supporting electrolyte, no electrochemical response for the Ni(II/III) couple or the polypyrrole backbone was observed after five potential scans. Upon transfer of the electroinactive film to a solution containing perchlorate anion, electroactivity was partially restored. Tight ion-pairing of the p-toluenesulfonate anion with the metal complex would restrict ion motion within the film and could account for the loss of electroactivity. Alternatively, the large size of the p-toluenesulfonate anion might prevent its incorporation into the film during potential cycling.

There does not appear to be a clear explanation for the loss of electroactivity for these films. Examination of the electrode under an optical microscope after extended potential cycling shows no obvious stripping of the film from the electrode surface. It is not possible to know if contact is being lost at the electrode surface/polymer film interface. Other polymer films with polypyrrole backbones show a similar loss of electroactivity when scanned to high positive potentials.

Conductivity associated with the polypyrrole does not appear to affect the electrochemistry of the Ni(II/III) couple. The redox hopping conduction responsible for the metal wave therefore is independent of other electrochemistry occurring in the polymer film. Additional evidence for the separation of conductivities in the film comes from the voltammetry of thick polymer films. The polypyrrole oxidation wave is adjacent to the Ni(II/III) oxidation wave in the thick films (Figure 6). A comparison of the wave shapes for the metal oxidation/reduction in Figures 3 and 6 reveals no significant differences. These observations justify, we believe, the use of the charge under the Ni(III/II) reduction wave as a reliable measure of the surface coverage. Unfortunately we have been unable to

(21) (a) Osaka, T.; Naoi, K.; Organo, S. *J. Electrochem. Soc.* **1988**, *135*, 1071. (b) Warren, L. F.; Anderson, D. P. *Ibid.* **1987**, *134*, 101. (c) Shimidzu, T.; Ohtani, A.; Iyoda, T.; Honda, K. *J. Electroanal. Chem.* **1987**, *224*, 123. (d) Hyodo, K.; MacDiarmid, A. G. *Synth. Met.* **1985**, *11*, 167. (e) Salmon, M.; Diaz, A. F.; Logan, A. J.; Krounbi, M.; Bargon, J. *Mol. Cryst. Liq. Cryst.* **1982**, *83*, 265.

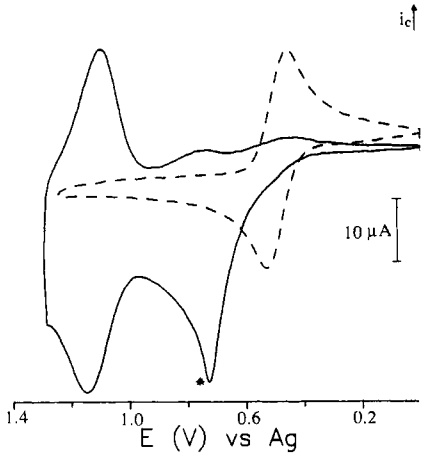

Figure 7. Voltammetric response of a polymer film of poly-Ni[14]C2pyrrole in 0.1 M $[(n\text{-Bu})_4N][ClO_4]/CH_3CN$ at 50 mV/s containing ferrocene. The peak marked with an asterisk is the mediated oxidation of ferrocene. Curve (---) is ferrocene at bare Pt electrode under the same experimental conditions; E vs Ag.

Table II. Effect of Anion and Solvent on Γ_{app}

anion[a]	compound	$10^9\Gamma_{app}$, mol/cm^2	
		CH_3CN[b]	CH_2Cl_2[e]
$[PF_6]^-$	Ni[14]C2pyrrole	*c*	3.9[f]
	Ni[14]C3pyrrole	0.7	
	Ni[14]C6pyrrole	7.1	5.6[f]
$[SO_3CF_3]^-$	Ni[14]C2pyrrole	*d*	5.8[f]
	Ni[14]C3pyrrole	4.8	
	Ni[14]C6pyrrole	12.1	13.8
$[BF_4]^-$	Ni[14]C2pyrrole	0.5	8.4[f]
	Ni[14]C3pyrrole	8.5	
	Ni[14]C6pyrrole	6.4	9.4
$[ClO_4]^-$	Ni[14]C2pyrrole	6.9	4.7[f]
	Ni[14]C3pyrrole	19.1	
	Ni[14]C6pyrrole	21.4	10.9

[a] 0.1 M $[(n\text{-Bu})_4N][anion]$. [b] 1.12–1.22 mM, 40 polymerization scans. [c] No polymerization detected. [d] Film too thin for accurate measure of Γ_{app}. [e] 1.1–0.9 mM 10 and 15 polymerization scans for Ni[14]C6pyrrole and Ni[14]C2pyrrole, respectively. [f] Inaccurate concentrations due to limited solubilities.

selectively degrade the polypyrrole electrochemistry to conclusively show that the redox hopping is independent of any other conduction mechanisms that may be occurring in these films.

The addition of ferrocene to a solution in which a poly-Ni[14]C2pyrrole film is placed (0.1 M $[(n\text{-Bu})_4N][ClO_4]/CH_3CN$ and no Ni[14]C2pyrrole) exhibits mediation of the ferrocene/ferricinium couple by the polypyrrole portion of the polymer (Figure 7). Polypyrrole is thus capable of efficiently transferring an electron to a solution species. The films are essentially pinhole free as only a very small direct oxidation wave for ferrocene at the Pt electrode is detected. A correspondingly small reduction wave for the ferricinium cation on the return scan is observed. No reducing agents present in the polymer film, Ni(II) and polypyrrole(0), have potentials sufficiently negative to reduce the cation in an electromediated fashion, so a reductive current burst analogous to the oxidation is not detected.

Anion Effects. The anion used in the supporting electrolyte had an unexpectedly large effect on polymer film formation. The dependence of Γ_{app} on the supporting electrolyte anion is shown in Table II for the three different complexes. The polymerizations were performed on 1.12–1.22 mM solutions by 40 repetitive potential cycles 200 mV past the Ni(II) oxidation wave. Polypyrrole formation is somewhat dependent on the supporting electrolyte anion, although the effects are not large. However, recent experiments using a quartz crystal microbalance demonstrate that the efficiency of polypyrrole formation (surface coverage) in CH_3CN can decrease by 25% when changing the electrolyte from $LiClO_4$ to $[(n\text{-Bu})_4N][BF_4]$.[22]

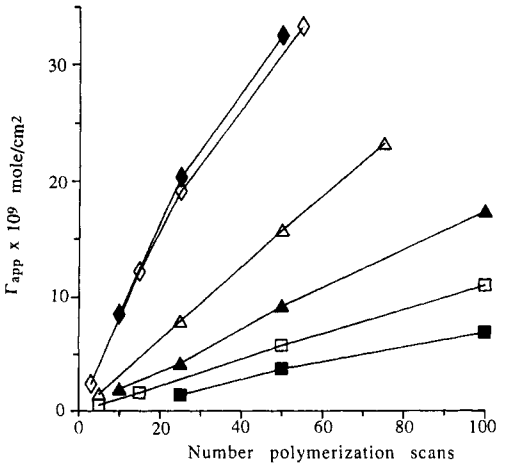

Figure 8. Apparent surface coverage (Γ_{app}) as a function of the number of polymerization scans for a given monomer concentration: poly-Ni[14]C6pyrrole (◇) 1.9 mM, (△) 0.72 mM, (□) 0.25 mM; poly-Ni[14]C2pyrrole (◆) 3.56 mM, (▲) 1.24 mM, (■) 0.53 mM. Γ_{app} measured at 50 mV/s. All films grown at 100 mV/s, scan range from 0 to 1.45 V [150 mV past the Ni(II/III) oxidation] in 0.1 M $[(n\text{-Bu})_4N][ClO_4]/CH_3CN$; E vs Ag.

Perchlorate anion yielded the most rapid polymerization for all of the monomers investigated. The Γ_{app} decreases by a factor of about 3 for poly-Ni[14]C6pyrrole when either the $[BF_4]^-$ or $[PF_6]^-$ anion replaced perchlorate. An even greater difference is observed for poly-Ni[14]C3pyrrole when changing from perchlorate to hexafluorophosphate, where the apparent surface coverage decreases by a factor of almost 30. The decrease is most dramatic for poly-Ni[14]C2pyrrole, where in the presence of $[PF_6]^-$ no polymerization was observed under any circumstances. Note that Ni[14]C2pyrrole does form a very thin polymer film in a triflate/acetonitrile medium, but the error in measuring Γ_{app} is large; films of reasonable thickness $\Gamma_{app} \sim 10^{-9}$ mol/cm^2 could be grown in $[SO_3CF_3]^-$ electrolyte, but more positive potentials were required. Unfortunately the effects of a given anion are not always predictable; note the Γ_{app} for the poly-Ni[14]C6pyrrole film in triflate supporting electrolyte appears to be high relative to the results obtained on the two other macrocyclic complexes.

Polymerization of 1-(2-(acetylamino)ethyl)pyrrole, IIa, was performed in both perchlorate and hexafluorophosphate supporting electrolytes. No anion effects were observed; films grew at similar rates. The compound 1-(2-aminoethyl)pyrrole, IIIa, did not electropolymerize under the conditions employed to form either the transition-metal complex polymer films or those formed from IIa. The inability to electropolymerize pyrrole in the presence of basic species is known.[20b,23] These results unfortunately do not aid in understanding the polymerization behavior of the transition-metal complexes. However, the interactions of the various anions with the metal/pyrrole complex must therefore be significantly different from those with the substituted pyrrole itself.

Monomer Effects. Polymerization rates and resulting film thicknesses are dependent on the monomer. Figure 8 demonstrates the dependence of Γ_{app} on the monomer

(22) Baker, C. K.; Reynolds, J. R. *J. Electroanal. Chem.* **1988**, *251*, 307.
(23) Morse, N. J.; Rosseinsky, D. R.; Mortimer, R. J.; Walton, D. *J. Electroanal. Chem.* **1988**, *255*, 119.

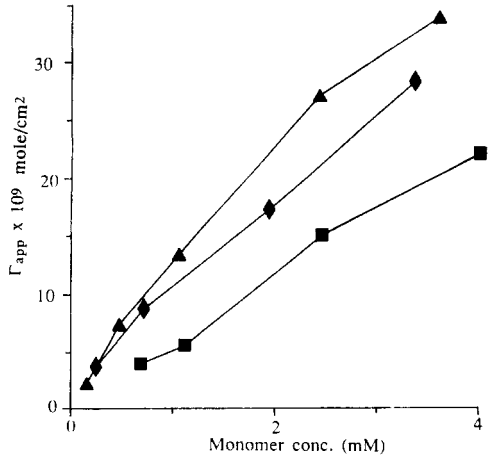

Figure 9. Apparent surface coverage (Γ_{app}) as a function of the monomer: (▲) poly-Ni[14]C3pyrrole; (◆) poly-Ni[14]C6pyrrole; (■) poly-Ni[14]C2pyrrole. Γ_{app} measured at 50 mV/s. All films grown for 25 repetitive potential scans, 100 mV/s, scan range from 0 to 1.48 V [200 mV past the Ni(II/III) oxidation] in 0.1 M $[(n\text{-Bu})_4N][ClO_4]/CH_3CN$; E vs Ag.

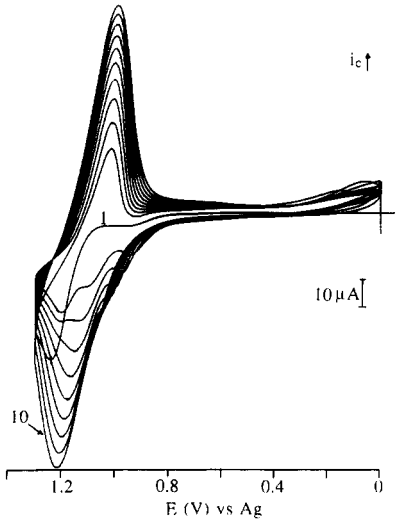

Figure 10. Electropolymerization of a 1.14 mM solution of Ni[14]C6pyrrole at Pt electrode in CH_2Cl_2; υ = 100 mV/s, E vs Ag and 0.1 M $[(n\text{-Bu})_4N][BF_4]$.

concentration used to grow the polymer film. All polymerizations were performed by 40 repetitive cycles 200 mV past the Ni(II) oxidation peak. The poly-Ni[14]C3pyrrole and poly-Ni[14]C6pyrrole film surface coverages are similar, although the poly-Ni[14]C3pyrrole films are consistently higher. The poly-Ni[14]C2pyrrole films are not as thick as those prepared from the other monomers by about a factor of 2. The difference in Γ_{app} is not due to electrochemical inactivity for a portion of the poly-Ni[14]-C2pyrrole film as the current–potential curves measured during the film growth stage for Ni[14]C2pyrrole indicate a much slower increase in both the oxidative and reductive currents from the Ni(II/III) couple when compared to similar solutions of either Ni[14]C3pyrrole or Ni[14]C6-pyrrole.

Shown in Figure 9 is a plot of coverage versus number of polymerization scans for polymer films grown from three different concentration solutions of each of compounds Ni[14]C2pyrrole and Ni[14]C6pyrrole. All polymerizations were carried out by repetitively cycling 150 mV past the Ni(II) oxidation wave. For both compounds the Γ_{app} is related linearly to the number of polymerization scans at the two low concentrations. However, note that it requires a less concentrated solution of the compound Ni[14]C6-pyrrole to attain a similar surface coverage to Ni[14]C2-pyrrole. At a concentration of 1.9 mM for Ni[14]C6pyrrole and 3.6 mM for Ni[14]C2pyrrole polymer, film growth ceases after approximately 55 potential scans. Continued potential cycling leads to no further increase in the measured currents and eventually the currents begin to decrease. The plots, Figure 9, for the high concentration solutions show lower than expected Γ_{app}, based on extrapolation from the low surface coverage data, after approximately 25 polymerization scans. A decrease in both the efficiency of monomer oxidation and coupling of the oxidized monomer to the polymer film surface as well as formation of soluble oligomers could account for the observed cessation of film growth in the case of thick films. The data presented in Figures 4, 8, and 9 implicate different "rate constants" or polymerization efficiencies for the different metal complex monomers.

Steric encumbrance and coulombic repulsions are two factors that can explain the observed results with the macrocyclic complexes. Since the macrocyclic complexes are saddle shaped[14] rather than planar, there may be a steric encumbrance component to the approach of two or more of the pyrrole moieties upon oxidation when the alkyl chain is only two methylene units long. The higher apparent surface coverages for the three and six methylene spacers implies a greater flexibility of orientations in which the macrocycles can approach each other. Coulombic repulsions might also arise as the cationic monomers approach each other to couple onto a polycationic film. Extending the alkyl chain should lower the relative coulombic repulsions. We are presently investigating both the effect of alkyl chain length and complex charge in some related complexes so that a better understanding of the chemistry that is occurring in the polymer films described herein can be attained.

Solvent Effects. The electrochemical properties of the Ni[14]C2pyrrole and Ni[14]C6pyrrole complexes in CH_2Cl_2 were also investigated. It was of particular interest to determine if anion effects similar to those observed in CH_3CN were encountered in methylene chloride during electropolymerization. The polymer film growth characteristics are somewhat different in CH_2Cl_2 than in acetonitrile. Shown in Figure 10 is the electropolymerization of Ni[14]C6pyrrole at a Pt electrode with Ag wire reference, 1.14 mM metal complex, and 0.1 M $[(n\text{-Bu})_4N][BF_4]$ in CH_2Cl_2 (compare with Figure 2). The first four scans display complicated electrochemistry for the oxidative currents. Subsequent potential scans (5 through 10) give current–potential curves that appear similar to those observed for electropolymerization in the acetonitrile media. The data indicate that the electrochemistry of the macrocycle is irreversible on the Pt electrode but reversible on the polymer film surface. Changes in the supporting electrolyte anion ($[ClO_4]^-$, $[PF_6]^-$, or $[SO_3CF_3]^-$) do not alter substantially the current-potential curves shown in Figure 10. Ni[14]C2pyrrole is less soluble than Ni[14]C6pyrrole in methylene chloride, and slower polymer film growth rates are observed. However, the details of film growth are analogous for the two monomers.

The film-coated electrodes were examined in 0.1 M $[(n\text{-Bu})_4N][BF_4]/CH_3CN$ containing no monomer. Solvent plays no role in the studying the electrochemical response of the polymer film once it is formed. Electrochemical properties of the films prepared in CH_2Cl_2 are virtually indistinguishable from those prepared in acetonitrile. The broad oxidation and reduction waves at ~800 mV vs Ag wire provide evidence for a polypyrrole backbone, and the metal-centered waves are also well defined. Presented in

Scheme II

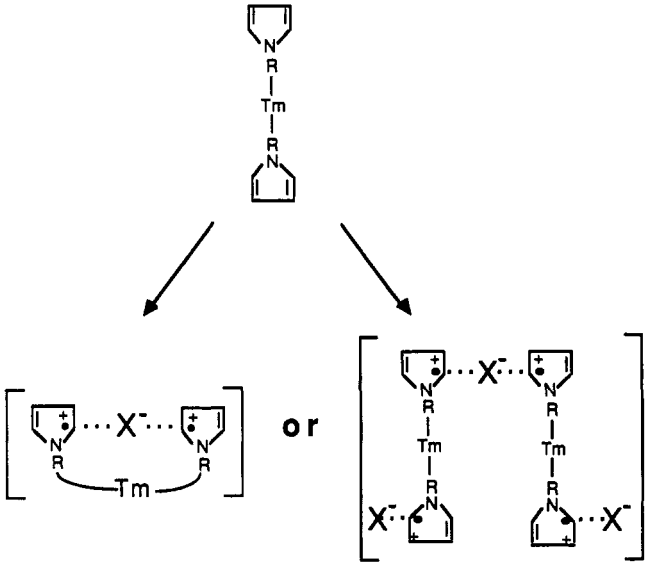

Tm = Ni[14] macrocycle

R = alkyl chain

Table II are the apparent surfaces coverages measured for the two monomers, 10 and 15 polymerization scans for Ni[14]C6pyrrole and Ni[14]C2pyrrole, respectively. The large anion effects seen for electropolymerization in CH_3CN are virtually nonexistent in CH_2Cl_2. The lower Γ_{app} observed for poly-Ni[14]C6pyrrole grown in $[PF_6]^-$ electrolyte likely arises from the lower solubility of the monomer in that electrolyte than in the other supporting electrolytes. Apparent surface coverages for poly-Ni[14]C2pyrrole are artificially low because of limited solubility of the monomer in all electrolytes. Note that the Γ_{app} values for films grown in CH_2Cl_2 for 10 or 15 scans are in some instances greater than those for the analogous film grown in CH_3CN for 40 potential scans. Solvent influences on polypyrrole film growth have been detected by using the quartz crystal microbalance.[22]

The data presented in Table II strongly implicate ion-pairing in acetonitrile as a major factor in the electropolymerization chemistry. Apparently ion-pair formation is less important for the polymerization chemistry in methylene chloride. Since anion and chain-length dependences are detected during the electropolymerization reaction, chelation of the anion by the metal complex is implicated as the cause for the observed behavior. Strong ion-pairing inhibits the radical coupling reaction necessary for polypyrrole formation. The nature of the ion-paired species may resemble either of the two possible structures depicted in Scheme II. However, further speculation as to the nature of this ion-paired species is not reasonable at this time. We are preparing new metal complexes containing the various pyrrole ligands in order to understand the ion-pairing behavior in more detail and molecular modeling studies are also in progress.

Conclusion

The data presented herein further demonstrate the usefulness of pendant pyrrole groups as electropolymerizable moieties for preparing transition-metal complex polymer films. The dependence of film growth on the distance between the polymerizable moiety and the metal complex and small supporting electrolyte anions are observations that have not been previously commented upon. The change in electrochemical behavior observed for the polypyrrole when changing anions is an intriguing result especially if observable in other polymer films. The implication is that the internal constitution of the polymer film and possibly the ionic, redox hopping, and electronic conduction mechanisms can be controlled by minor changes in the conditions under which the polymer films are probed. We expect that these observations will be applicable to a number of related polymer films. Finally, the large role that anions play in the electropolymerization chemistry was unexpected. While the anion chelation phenomenon is still speculative, it may be more generally applicable to explaining the film growth characteristics of other monomer systems.

Acknowledgment. This work was supported in part by the Defense Advanced Research Projects Agency through a grant monitored by the Office of Naval Research. We thank Professor Jody G. Redepenning (RPI) for insightful discussions, Professor George Gokel (University of Miami) for suggesting the anion chelation phenomenon, and Joseph P. McIsaac (RPI) for kindly supplying the computer programs used in manipulating the digital electrochemical data.